

Effect of Silica on the Thermal Degradation of Poly(vinyl butyral)

Robert L. White* and Aurobindo Nair

Department of Chemistry and Biochemistry, University of Oklahoma,
Norman, Oklahoma 73019

Received July 16, 1990

Thermal degradation of poly(vinyl butyral) (PVB) coated on silica is investigated. Degradation products for PVB and PVB in contact with silica are identical. However, temperature profiles for volatile species produced from PVB/silica mixtures are shifted to higher temperature by 60 °C relative to the profiles for the same species evolved from PVB. The inhibitory effect of silica on PVB degradation is attributed to interactions between polymer hydroxyls and silanol groups on the silica surface.

Introduction

Polymers are used in the ceramics industry to facilitate handling and machining of ceramic "green bodies" prior to sintering. Ideally, polymer binders completely decompose or "burn out" well below temperatures required for ceramic sintering and thus have no effect on the sintering process. Unfortunately, this may not be the case, especially if sintering in nonoxidative atmospheres is required, as is sometimes necessary for production of ceramics for use in electronics applications.¹⁻⁴

This paper describes investigations of the thermal degradation of commercial grade poly(vinyl butyral) (PVB), which is commonly employed as a binder for making electronic ceramics. Thermal degradation of PVB and PVB coated on silica are compared. PVB/silica mixtures containing 8% by weight PVB were prepared to simulate composition of green bodies typically used in making ceramics for electronics. Thermal degradation in flowing helium was studied by pyrolysis GC/MS and pyrolysis GC/FT-IR. In addition, DRIFTS/MS, a new thermal analysis technique developed in our laboratory,⁵ was employed to study thermal degradation of PVB in high vacuum. DRIFTS/MS comprises a combination of diffuse reflectance Fourier transform infrared spectroscopy (DRIFTS) and mass spectroscopy (MS). By use of this apparatus, polymer residue was monitored by diffuse reflectance infrared spectroscopy, while mass spectroscopy was used to detect volatile products generated during thermal degradation. This apparatus was used to compare the thermal degradation of PVB with PVB in contact with silica while a heating ramp of 8.6 °C/min was applied to samples to simulate sintering conditions.

Experimental Section

Apparatus. Pyrolysis/gas chromatography experiments were performed by using a microfurnace pyrolyzer built in our laboratory.⁶ For PVB pyrolysis, samples were prepared by dissolving PVB in 1-butanol, depositing this solution on the pyrolysis probe tip by using a syringe, and evaporating the solvent by gentle heating with a heat gun. Slurries containing silica or silanized silica (vide infra) suspended in PVB/1-butanol solution were made to obtain pyrograms of PVB coated on these solids. Slurries were prepared so that deposited solids contained approximately 8% PVB by weight after solvent evaporation. Sample sizes ranging

between 2 and 50 µg were employed for all separations. The pyrolysis oven was interfaced to a Hewlett-Packard (Palo Alto, CA) 5980A capillary gas chromatograph. A 25 m × 0.32 mm i.d. Hewlett-Packard Ultra-1 column with 0.52-µm cross-linked methyl silicone gum stationary phase was used for all separations. A helium carrier gas flow rate of 5 mL/min and a temperature program starting with a 1 min isothermal period at 30 °C followed by a 5 °C/min ramp to 190 °C were employed for all separations.

GC/MS detection of pyrolysis products was facilitated by interfacing the gas chromatograph to a Hewlett-Packard 5985 quadrupole mass spectrometer. GC/MS spectra were acquired at a rate of 20 spectra/min. Electron impact mass spectra were obtained by using a 70-eV ionization potential and scanning from m/z 15 to 500. Chemical ionization mass spectra were obtained by using a 250-eV ionization potential with 0.8 Torr of methane in the ion source and scanning from m/z 42 to 500. Mass spectral library searches employed a 38 000-spectra NBS mass spectral library.

GC/FT-IR spectra were obtained by interfacing a Mattson Instruments Inc. (Madison, WI) Sirius 100 FT-IR to the gas chromatograph via a light pipe interface constructed in our laboratory. This interface consisted of a 7-in.-long gold-coated light pipe, three off-axis parabolic mirrors, and a liquid nitrogen cooled MCT detector mounted in a dry air purged enclosure placed between the FT-IR and gas chromatograph.⁷ GC/FT-IR spectra were acquired at 8-cm⁻¹ resolution at a rate of 20 spectra/min. Infrared spectra were searched against the 3300-spectra EPA vapor-phase infrared library.

DRIFTS/MS experiments were performed by using an apparatus built in our laboratory that consists of an interface between the FT-IR equipped with an evacuable diffuse reflectance environmental chamber and the quadrupole mass spectrometer. The DRIFTS/MS apparatus is described in detail elsewhere.⁵ During DRIFTS/MS analysis samples were heated from 50 to 550 °C at a rate of 8.6 °C/min in vacuum below 1×10^{-7} Torr. DRIFTS spectra were acquired at 1-min intervals by signal averaging 400 scans at 8-cm⁻¹ resolution. Diffuse reflectance spectra were converted to apparent absorbance format $\{\log (1/R)\}$ ⁸ prior to display or subtraction. Apparent absorbance was chosen instead of the Kubelka-Munk format because it is less sensitive to spectral baseline offsets. Mass spectra were obtained at 0.5-min intervals over a mass range from m/z 15 to 500. Electron impact spectra were obtained with minimal fragmentation by employing a 20-eV ionizing potential.

Reagents. Samples of poly(vinyl butyral) (PVB) and silica employed to make ceramic green bodies were obtained from Hitachi, Ltd. (Hitachi-shi, Japan), and were used without purification. Commercial grade PVB is prepared by converting poly(vinyl acetate) to poly(vinyl alcohol), which is subsequently reacted with butanal. This process does not lead to complete

(1) Otsuka, K.; Usami, T.; Sekibata, M. *Yogyo Kyokaishi* 1981, 89, 37.

(2) Otsuka, K.; Ogihara, S. *Yogyo Kyokaishi* 1984, 92, 210.

(3) Otsuka, K.; Ogihara, S. *Yogyo Kyokaishi* 1984, 92, 629.

(4) Otsuka, K.; Ogihara, S. *Yogyo Kyokaishi* 1985, 93, 28.

(5) White, R. L. *J. Anal. Appl. Pyrolysis*, in press.

(6) White, R. L. *J. Anal. Appl. Pyrolysis*, in press.

(7) White, R. L. *Chromatography/Fourier Transform Infrared Spectroscopy and Its Applications*; Marcel Dekker: New York, 1990; p 59.

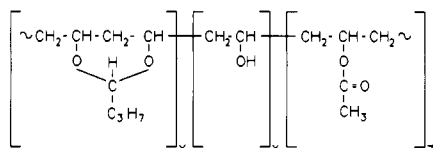
(8) Kortum, G. *Reflectance Spectroscopy*; Springer-Verlag: New York, 1969; p 59.

Table I. 900 °C PVB Pyrolysis Products

GC peak	ret time, min		% ^b	MW ^c	search results		
	MS ^a	IR			MS	IR	probable identity
1	0.92	1.39	22.90		CO, CO ₂ , alkenes	CO, CO ₂ , alkenes	CO, CO ₂ , alkenes
2	1.38	1.98	5.6	66	unsatd hydrocarbon	unsatd hydrocarbon	unsatd hydrocarbon
3	1.60	2.29	3.6	72	butanal	butanal	butanal
4	2.20	2.71	6.4	80	unsatd hydrocarbon	unsatd hydrocarbon	unsatd hydrocarbon
5	2.41	3.33	19.8	78	benzene	benzene	benzene
6	4.30	5.40	9.1	92	toluene	toluene	toluene
7	6.81		1.6	106	xylylene		xylylene
8	7.07		1.0	106	xylylene		xylylene
9	7.58	8.54	5.8	104	styrene	benzene deriv	styrene
10	12.19		3.1	116	benzene deriv		benzene deriv
11	16.50	16.77	6.2	128	naphthalene	naphthalene	naphthalene

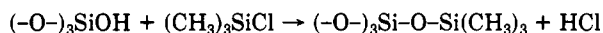
^a GC/MS electron impact retention time. ^b Percentage of GC/MS electron impact total ion current. ^c Based on detection of the chemical ionization M + H ion.

conversion to poly(vinyl butyral) but instead results in a material containing residual acetate and hydroxyl groups:



The composition of the PVB used for experiments described here was $X > 75\%$, $Y = 18\text{--}22\%$, and $Z < 3\%$. Infrared spectra of this material contained a medium-intensity O-H stretching band at 3540 cm^{-1} and a small C=O stretching vibration band at 1736 cm^{-1} , which is consistent with this composition. Silica used for studies described here was characterized by a $1\text{-}\mu\text{m}$ average particle size and $16.7\text{ m}^2/\text{g}$ surface area. 1-Butanol solvent was purchased from EM Science (Gibbstown, NJ) and was not further purified prior to use. Chlorotrimethylsilane was obtained from Aldrich Chemical Co. (Milwaukee, WI) and was also used without further purification. High-purity methane obtained from Union Carbide, Linde division (Somerset, NJ), was used for the mass spectrometric chemical ionization reagent. Diamond powder employed as diluent for DRIFTS/MS experiments was purchased from Johnson Matthey/AESAR (Seabrook, NH). Contaminants in diamond powder were removed by heating the powder to 500°C under a 10^{-1} -Torr vacuum for 4 h. Potassium bromide (KBr) powder employed to obtain background interferograms was prepared by crushing scraps of high-purity window material with a mortar and pestle. KBr powder was calcined by heating at 550°C for 5 h in flowing air.

Silanized silica was made from silica by reaction with chlorotrimethylsilane. Approximately 1 g of silica was heated in a quartz tube under vacuum at 1000°C for 4 h. This promoted condensation of hydrogen-bonded SiOH surface groups and facilitated removal of organic impurities. The thermally treated silica was then placed into a round-bottom flask containing 15 mL of chlorotrimethylsilane, and the mixture was refluxed for 16 h. Surface OH groups remaining after thermal treatment were replaced by nonpolar silyl groups by reaction with chlorotrimethylsilane:



Removal of hydroxyl groups was verified by comparing a diffuse reflectance infrared spectrum of silica with a spectrum obtained from the silanized silica. The DRIFTS spectrum of the silanized material exhibited significantly lower absorbance in the $3800\text{--}2500\text{-cm}^{-1}$ region compared to the DRIFTS spectrum of untreated silica. The surface area of the silanized silica was $10.6\text{ m}^2/\text{g}$.

Results

Pyrolysis Gas Chromatography. Pyrolysis gas chromatography combined with infrared and mass spectrometric detection was employed to generate and identify thermal degradation products from PVB and PVB coated on silica and silanized silica. Pyrolysis below 400°C resulted in broad chromatographic elutions, indicating that

the degradation process was slow at these temperatures. Pyrograms obtained below 400°C contained severely overlapping elutions and were not easily interpreted. Above 400°C , narrow chromatographic elutions were routinely obtained. PVB was pyrolyzed in flowing helium at 500 and 900°C to investigate the effect of temperature on degradation product distributions. By correlation of results from chemical ionization and electron impact pyrolysis GC/MS with vapor-phase infrared spectra obtained from pyrolysis GC/FT-IR, many PVB degradation products generated at 900°C were identified (Table I). Major products at 900°C included CO, CO₂, benzene, and toluene. Other degradation products were unsaturated organic species, and most of these were aromatic. Butanal was detected in 900°C pyrograms but represented only 3.6% of the integrated total ion current in the electron impact GC/MS pyrogram.

Pyrolysis of PVB at 500°C resulted in a different product distribution. Sixteen degradation products constituting over 90% of the integrated total ion current in the 500°C electron impact pyrogram were characterized by mass spectral and infrared vapor-phase library searches. The results of pyrolysis GC/MS and pyrolysis GC/FT-IR analyses are compiled in Table II. Butanal was the major pyrolysis product at 500°C . Benzene, a major product at 900°C , was formed in small amounts at 500°C . Other significant products at 500°C contained carbonyl functionalities in the form of either aldehydes or ketones. Search results indicated that several degradation products were unsaturated.

To test the influence of silica on the thermal degradation of PVB, solutions containing 8% PVB and 92% silica or silanized silica after evaporation of 1-butanol solvent were deposited on the pyrolysis probe tip and analyzed by pyrolysis GC/MS and pyrolysis GC/FT-IR. No discernible differences in degradation products or their relative amounts were detected after comparing results from pyrolysis of PVB, PVB/silica, and PVB/silanized silica at either 900 or 500°C .

DRIFTS/MS Analysis. Thermal degradation of PVB and PVB coated on silica and silanized silica was examined by DRIFTS/MS analysis during application of an $8.6^\circ\text{C}/\text{min}$ linear heating rate from 50 to 550°C and while the sample was maintained under vacuum ($<1 \times 10^{-7}$ Torr). Diffuse reflectance infrared spectra of the solid residue and mass spectra of volatile degradation products were measured simultaneously during sample heating. Infrared spectral changes accompanying thermal degradation of PVB were identified by subtracting the spectrum obtained at 50°C from spectra obtained at higher temperatures. The difference spectra computed in this manner contained infrared changes resulting from sample heating.

Table II. 500 °C PVB Pyrolysis Products

GC peak	ret time, min		% ^b	MW ^c	search results		probable identity
	MS ^a	IR			MS	IR	
1	0.93	0.98	26.0	44	CO, CO ₂ , H ₂ O, acetaldehyde	CO, CO ₂ , H ₂ O, acetaldehyde	CO, CO ₂ , H ₂ O, acetaldehyde
2	1.09	1.18	1.4	58	acetone	acetone	acetone
3	1.45	1.54	1.1	70	2-unsatd aldehyde	aldehyde	unsatd aldehyde
4	1.51	1.69	41.6	72	butanal	butanal	butanal
5	2.08	2.20	13.6	70	2-butenal	aldehyde	2-butenal
6	2.24		0.2	78	benzene		benzene
7	2.40	2.51	2.0	84	4-penten-2-one	2-ketone	4-penten-2-one
8	2.50	2.68	1.1	84	3-penten-2-one	ketone	3-penten-2-one
9	2.92		0.1	60	acetic acid		acetic acid
10	3.34		1.0	84	unsatd hydrocarbon or ketone		unsatd hydrocarbon or ketone
11	6.01	6.18	0.4	96	2,4-hexadienal	aldehyde	unsatd aldehyde
12	9.03	8.83	1.7	106	benzaldehyde	benzaldehyde	benzaldehyde
13	12.42	11.95	0.6	120	arom ketone	ketone	arom ketone

^a GC/MS electron impact retention time. ^b Percentage of GC/MS electron impact total ion current. ^c Based on detection of the chemical ionization M + H ion.

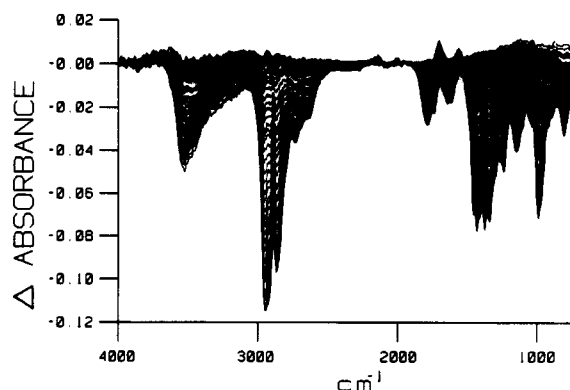


Figure 1. Diffuse reflectance difference spectra derived from DRIFTS/MS analysis of PVB.

PVB. Figure 1 is a plot of all the infrared difference spectra derived from DRIFTS/MS analysis of PVB. Negative spectral features indicate species lost during heating whereas positive features denote species formed by heating. Loss of polymer hydroxyl groups was observed immediately after sample heating had begun. This was detected as a decrease in infrared absorbance in the 3650–3300-cm⁻¹ range, corresponding to O–H stretching, and a concomitant decrease in band intensity at 1140 cm⁻¹ for the C–OH stretching vibration. The absence of a negative absorbance band at 1640 cm⁻¹ corresponding to the H–O–H bending vibration indicated that no physisorbed water was present in the sample. This was expected because samples were evacuated at 50 °C under high vacuum (<1 × 10⁻⁷ torr) for at least 1 h prior to analysis. Figure 2a is the integrated apparent absorbance temperature profile for the O–H stretching vibration. This profile shows that most of the hydroxyl groups are lost prior to 400 °C, which is consistent with a previous thermogravimetric analysis of poly(vinyl alcohol).⁹ Hydroxyl group loss was most likely accompanied by generation of vapor-phase water. Unfortunately, the mass spectrometer was unable to distinguish water evolved from PVB degradation from water vapor desorbing from the heated metal sample holder. However, changes in infrared spectra indicated that hydroxyls were lost primarily by dehydration yielding CH=CH moieties in the solid residue. This was detected as a slight increase in absorbance at 3014 cm⁻¹ at the beginning of the temperature ramp corresponding to the (CH=C)H stretching vibration as well as an ab-

sorbance increase at 1590 cm⁻¹ due to C=C stretching. The initial increase in absorbance for the 3014 cm⁻¹ band was coincident with the O–H stretching vibration band intensity decrease. Hydrocarbon evolution was detected in diffuse reflectance infrared spectra by decreased intensity in the aliphatic C–H stretching region (3000–2800 cm⁻¹). Little change in absorbance was observed at low temperatures, but significant absorbance decreases occurred above 200 °C in this region of diffuse reflectance spectra (Figure 2b). A band at 1000 cm⁻¹ assigned to the –C–O–C–O– stretching vibration was found to decrease with increasing sample temperature in a manner similar to the C–H stretching vibration absorbance bands (Figure 2c). Figure 2d shows that the temperature profile for the CH₃ bending vibration band at 1377 cm⁻¹ was exactly the same as for the 1000-cm⁻¹ band. Methyl groups are present in the polymer only as part of butyral and acetate functionalities. Because the number of acetate groups was small, contributions to the temperature profile of this band from acetate loss were negligible. Thus, absorbances of the CH₃ bending and –C–O–C–O– stretching vibrations were selective measures of butyral functionality loss. The total integrated apparent absorbance temperature profile contained contributions from all changes occurring to the polymer residue due to heating. The total integrated apparent absorbance profile (Figure 2e) was similar to the –C–O–C–O– profile, suggesting that the major degradation path involved loss of butyral. Carbonyl formation and increasing polymer unsaturation were detected in infrared spectra by increased absorbance in the 1750–1550-cm⁻¹ region (Figure 1). The low frequency of the C=C vibration (1590 cm⁻¹) is indicative of conjugated unsaturation.¹⁰ Figure 2f shows that below 300 °C, the integrated apparent absorbance in the C=O and C=C stretching vibration regions increased as O–H and –C–O–C–O– stretching vibration bands decreased. Above 300 °C, the intensity of the C=O and C=C bands decreased, indicating that these moieties were being lost from the polymer residue.

DRIFTS/MS mass spectral results indicated that the major product of PVB thermal degradation was butanal. The electron impact total ion current temperature profile passed through a maximum at 317 °C, but significant ion intensity was also measured at temperatures above 400 °C (Figure 3a). The highest ion intensity was observed at *m/z* 44, which is the base peak in butanal mass spectra and the molecular ion of CO₂ and acetaldehyde. The DRIFTS/MS temperature profile for *m/z* 44 is shown in

(9) Montaudo, G.; Puglisi, C.; Scamporrino, E.; Vitalini, D. *J. Polym. Sci.: Polym. Chem. Ed.* 1986, 24, 301.

(10) Socrates, G. *Infrared Characteristic Group Frequencies*; Wiley: New York, 1980; p 32.

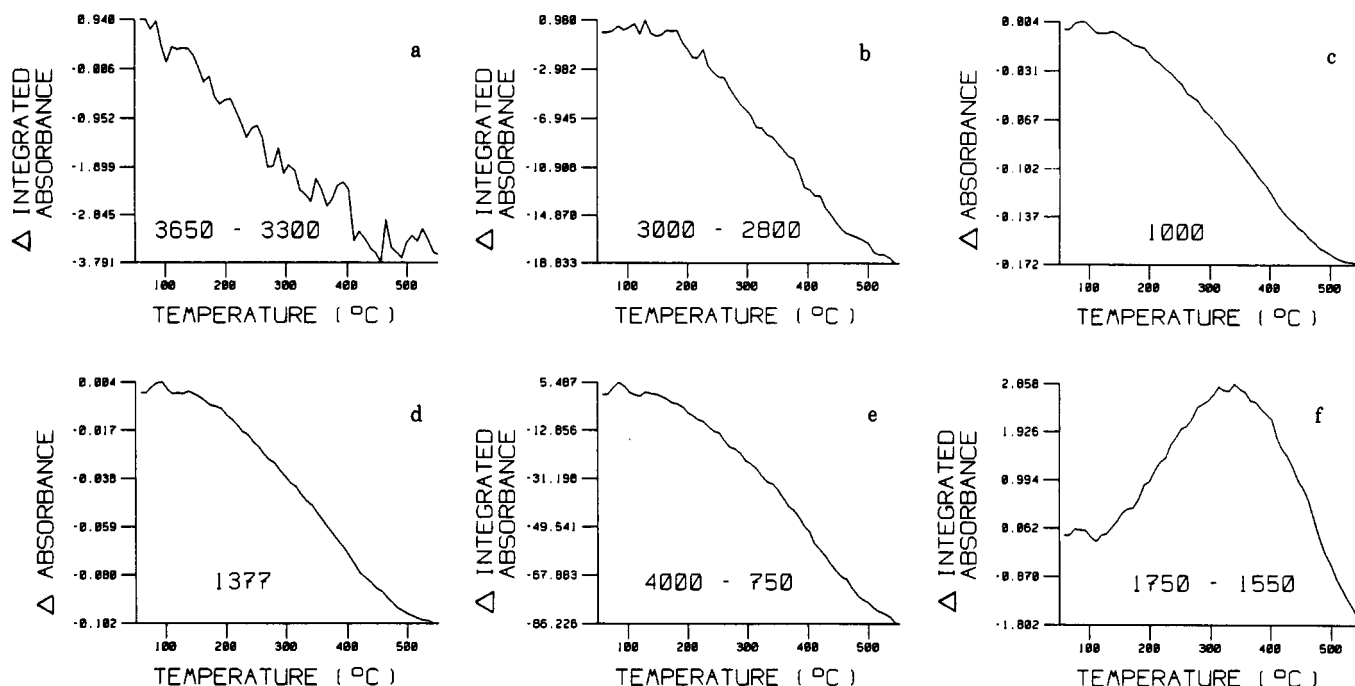


Figure 2. Temperature profiles for PVB degradation derived from DRIFTS/MS infrared measurements and representing various spectral regions and absorbance bands. Absorbance band locations or integration limits are given in cm^{-1} for each profile.

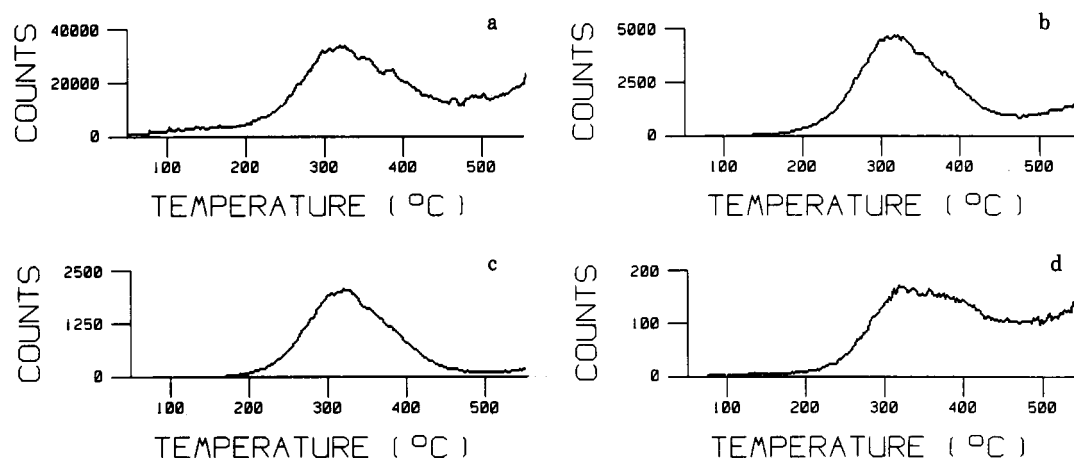


Figure 3. DRIFTS/MS mass spectral profiles for PVB degradation corresponding to (a) total ion current, (b) m/z 44, (c) m/z 72, (d) m/z 91.

Figure 3b. The butanal molecular ion (m/z 72) was also intense and had a temperature profile similar to the m/z 44 ion (Figure 3c). Ions suspected to be derived from unsaturated species typically exhibited temperature profiles that contained significant ion current above the maximum evolution temperature. For example, Figure 3d is the selected mass profile for m/z 91 (toluene) which, in contrast to the profile for m/z 72 (Figure 3c), exhibits significant ion intensity above 400 °C.

PVB/Silica and PVB/Silanized Silica. Samples of PVB coated on silica and silanized silica were subjected to the same DRIFTS/MS analysis conditions as PVB. Diffuse reflectance difference spectra computed by subtracting the 50 °C spectrum from the 550 °C spectrum for PVB/silica and PVB/silanized silica are shown in Figure 4. The high absorbance of Si–O–Si stretching vibrations led to absorbance saturation in the 1250–1000- cm^{-1} spectral range. Therefore, no information regarding PVB degradation was obtained in this region. Comparison of difference spectra in Figure 4 reveals that the PVB/silica spectrum contains features attributed to silanol groups on silica that are less obvious in the PVB/silanized silica

spectrum. The PVB/silica spectrum contains negative features in the 3500–2500- cm^{-1} spectral region that are caused by loss of hydrogen-bonded SiOH moieties from silica. A negative band at 910 cm^{-1} is representative of the Si–OH stretching vibration¹¹ and is strong in the PVB/silica spectrum but weak in the PVB/silanized silica spectrum.

Infrared and mass spectral temperature profiles for PVB/silica exhibited the same features as for PVB but were shifted to higher temperature relative to PVB profiles. For example, Figure 5 shows temperature profiles for the integrated absorbance in the CH stretching vibration region and for the electron impact m/z 72 ion current derived from DRIFTS/MS analysis of PVB/silica. These profiles are similar to those obtained for PVB (Figures 2b and 3c) but are shifted to higher temperature by about 60 °C. In contrast, temperature profiles for PVB/silanized silica were found to be indistinguishable from corresponding PVB profiles.

(11) Nair, A.; White, R. L. *Appl. Spectrosc.* 1990, 44, 69.

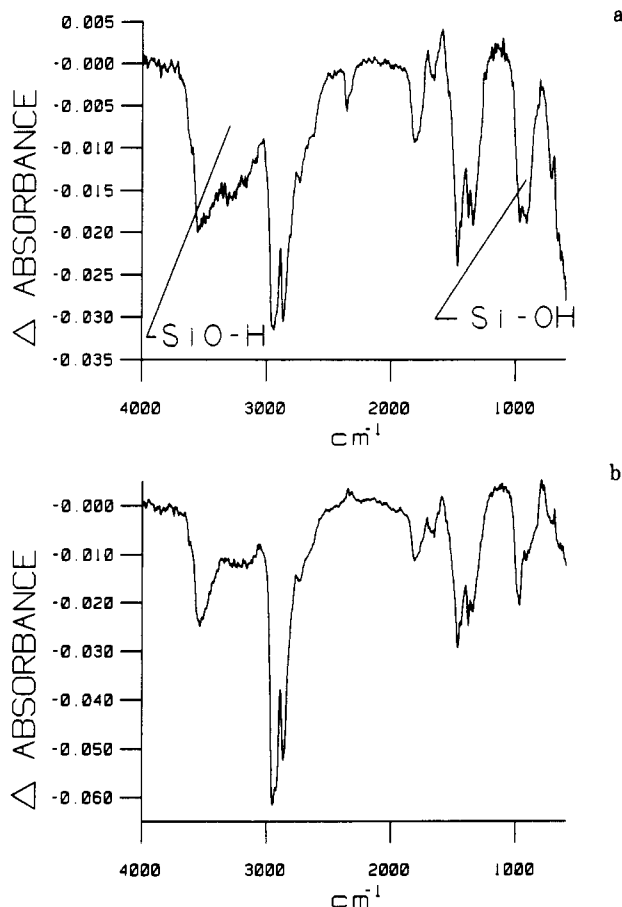


Figure 4. DRIFTS/MS difference spectra computed by subtracting the infrared spectrum obtained at 50 °C from the spectrum measured at 550 °C for (a) PVB coated on silica, (b) PVB coated on silanized silica.

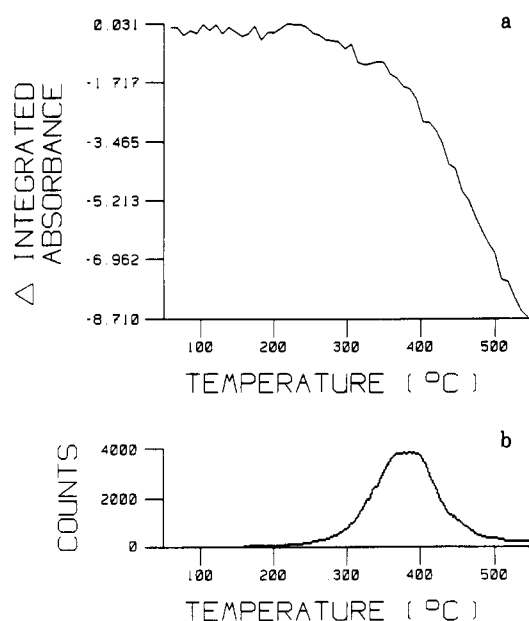


Figure 5. DRIFTS/MS temperature profiles for (a) changes in integrated infrared apparent absorbance between 3000 and 2800 cm^{-1} , (b) m/z 72 ion current.

Ions that were found in mass spectra obtained by pyrolysis GC/MS were also detected in DRIFTS/MS mass spectra. A list of some of these ions as well as their probable origins is compiled in Table III for PVB, PVB/silica, and PVB/silanized silica. Maximum evolution temperatures for ions detected by DRIFTS/MS analysis

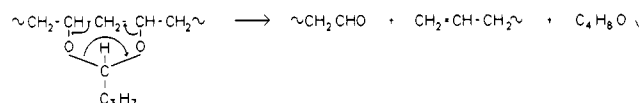
Table III. Maximum Evolution Temperatures

m/z	probable origin	$T_M, ^\circ\text{C}$		
		PVB	PVB and silica	PVB and silanized silica
44	CO_2 , acetaldehyde, butanal	317	380	320
58	acetone	298	380	320
60	acetic acid	341	380	310
70	2-butenal	322	380	320
72	butanal	317	380	320
78	benzene	325	380	328
84	3-penten-2-one	306	375	312
91	toluene	319	394	350
96	2,4-hexadienal	317	380	318
106	benzaldehyde	317	380	328

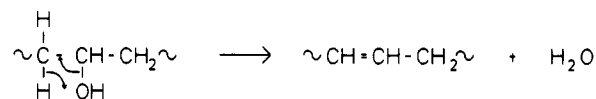
of PVB and PVB/silanized silica exhibited some variation but were typically near 320 °C. In contrast, maximum evolution temperatures for ions detected for the PVB/silica sample exhibited little variation and were typically at 380 °C.

Discussion

Analysis results from pyrolysis GC/MS and pyrolysis GC/FT-IR of PVB and PVB coated on silica and silanized silica were indistinguishable. Pyrolysis at 900 °C yielded primarily CO , CO_2 , and benzene. PVB degradation products produced at 900 °C are dictated by reaction product stability because sufficient energy is available to overcome most activation barriers.¹² Pyrolysis at 500 °C resulted in a degradation product distribution that was consistent with products detected by DRIFTS/MS. Pyrolysis and DRIFTS/MS results indicate that butanal formation is the major degradation process for PVB at temperatures between 200 and 400 °C. A intramolecular elimination mechanism has been proposed for production of butanal from PVB:¹³



Commercial grade PVB contains a large fraction of hydroxyl groups and some acetate functionalities in addition to butyral moieties. Therefore, a significant fraction of detected degradation products arise from reactions that do not involve butyral functionalities. For example, removal of hydroxyl groups via dehydration is a major thermal degradation mechanism between 100 and 400 °C because approximately 20% of the polymer is comprised of these functionalities:



DRIFTS/MS analysis was unable to detect water evolved from polymer dehydration because of the high water vapor background due to thermal desorption from heated vacuum system walls. However, water was detected as a pyrolysis product at 500 °C (Table II), and it is known that poly(vinyl alcohol) thermal degradation proceeds primarily via loss of water at temperatures below 300 °C.^{9,14} Acetate loss results in production of acetic acid,^{15,16} which was

(12) Lehrle, R. S.; Robb, J. C. *Nature* 1959, 183, 167.

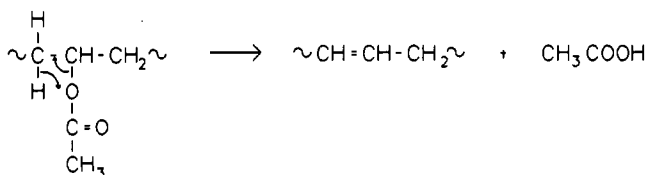
(13) Bakht, F. *Pakistan J. Sci. Ind. Res.* 1983, 26, 35.

(14) Gilbert, J. B.; Kipling, J. J. *Fuel* 1962, 12, 249.

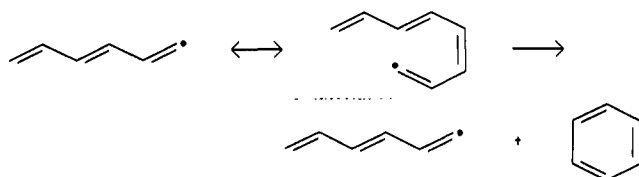
(15) Grassie, N. *Trans. Faraday Soc.* 1952, 48, 379.

(16) Ballisteri, A.; Foti, S.; Montauro, G.; Scamporrino, E. *J. Polym. Sci.: Polym. Chem. Ed.* 1980, 18, 1147.

detected in small quantities by pyrolysis and DRIFTS/MS measurements:

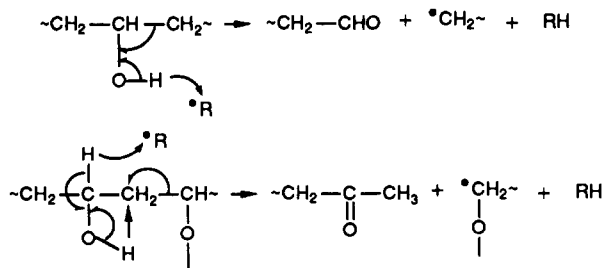


Intramolecular elimination reactions for butyral, hydroxyl, and acetate polymer groups all lead to polymer residue unsaturation. Polymer residue unsaturation was detected in DRIFTS spectra as increased infrared absorbance near 1600 cm^{-1} . Infrared absorption below 1650 cm^{-1} for C=C stretching vibrations indicates that the residue contained a significant amount of conjugated unsaturation. Polymer residue unsaturation led to generation of volatile unsaturated degradation products that were detected by pyrolysis at 500°C and were also indicated in mass spectra obtained by DRIFTS/MS. For example, benzene can be produced from polyene segments in the polymer residue by a radical mechanism.¹⁷



DRIFTS/MS mass spectral temperature profiles for m/z 78 and 91 showed that benzene and toluene evolution began at about 230°C . This indicates that significant conjugated unsaturation was present in the polymer residue at this temperature.

Some PVB degradation products contained both C=C and C=O moieties. This was confirmed by results from pyrolysis at 500°C and DRIFTS/MS analysis. Pyrolysis results identified acetaldehyde, 2-butenal, and 2,4-hexadienal as degradation products at 500°C . These substances are homologues with the common structure $\text{CH}_3(\text{CH}=\text{CH})_n\text{CHO}$. Ion intensity at m/z 44 (acetaldehyde, $n = 0$), m/z 70 (2-butenal, $n = 1$), and m/z 96 (2,4-hexadienal, $n = 2$) was detected in DRIFTS/MS mass spectra and probably resulted from these species. Homologues of the form $\text{CH}_3(\text{CH}=\text{CH})_n\text{COCH}_3$ (acetone, $n = 0$, and 3-penten-2-one, $n = 1$) were also detected in pyrolysis products at 500°C . Ions detected at m/z 58 and 84 in DRIFTS/MS spectra were probably due to these species. Homologues of structures $\text{CH}_3(\text{CH}=\text{CH})_n\text{CHO}$ and $\text{CH}_3(\text{CH}=\text{CH})_n\text{COCH}_3$ have previously been detected as thermal degradation products of poly(vinyl alcohol).⁹ Aldehyde and ketone moieties can be produced in the polymer residue from hydroxyl groups by free-radical hydrogen abstraction:



The intramolecular elimination mechanism proposed for

butanal evolution also leaves aldehyde functionalities in the polymer residue that may give rise to $\text{CH}_3(\text{CH}=\text{CH})_n\text{CHO}$ species.

Although thermal degradation products for samples of PVB coated on silica were identical with those detected for PVB, the temperature profiles for these species were different. Table III shows that temperatures corresponding to the maximum evolution of product were approximately 60°C higher when PVB was in contact with silica. However, when silica was treated to remove surface hydroxyls prior to coating with PVB (i.e., PVB/silanized silica), maximum evolution temperatures near those for PVB were obtained.

It is well-known that PVB adheres to oxide surfaces through hydroxyl-hydroxyl interactions.^{18,19} It is likely that $-\text{Si}-\text{O}-\text{C}-$ bridges were formed during thermal degradation of PVB in contact with silica by hydroxyl-silanol condensation reactions. No direct evidence for formation of $\text{Si}-\text{O}-\text{C}$ bonds was obtained by DRIFTS/MS because stretching vibrations for these species were obscured by intense $\text{Si}-\text{O}-\text{Si}$ stretching vibrations. However, if the polymer were chemically bonded to the silica surface at various points, a prerequisite for further degradation would be breakage of $\text{Si}-\text{O}-\text{C}$ links. This may explain why thermogravimetric analyses of PVB and PVB in contact with silica indicate that significantly more polymer residue remains at high temperature when silica is present.²⁰

Conclusions

In contrast to a recent report by Masia et al. that oxide powders catalyze PVB decomposition,²⁰ pyrolysis and DRIFTS/MS results described here indicate that under appropriate conditions PVB degradation can be inhibited by the presence of silica. Masia et al. compared thermogravimetric analysis curves for PVB and 2% PVB on silica and found that the weight loss profile for materials heated in argon containing 60 ppm oxygen were shifted to lower temperature by about 50°C when silica was present. Larger shifts were observed when samples were heated in air. DRIFTS/MS experiments described here were performed under high vacuum ($<1 \times 10^{-7}$ Torr), which can be considered an oxygen-free environment. In high vacuum, thermal degradation properties of PVB and PVB/silanized silica were found to be the same, indicating that catalysis did not occur. This implies that the presence of O_2 is a prerequisite for the catalytic effect of silica on PVB degradation and that small quantities of O_2 (60 ppm) are sufficient to cause this effect.

The inhibitory effect of silica on the thermal degradation of PVB is reported here for the first time. The fact that this effect has not been reported previously may indicate that the effect can be observed only under high vacuum conditions. If this is true, the inhibitory effect may be associated with removal of surface species present in air but absent in high vacuum. Physisorbed water is one surface species that would be expected to interact with PVB and is present on silica in air. Lack of infrared absorbance at 1640 cm^{-1} indicated that heating PVB/silica samples at 50°C under high vacuum for 1 h removed physisorbed water prior to DRIFTS/MS analysis. If the inhibitory effect of silica on the degradation of PVB under high vacuum can be attributed to interactions between polymer hydroxyls and silanol surface groups, the mag-

(18) Nakamae, K.; Sumiya, K.; Taii, T.; Matsumoto, T. *J. Polym. Sci.: Polym. Symp.* 1984, 71, 109.

(19) Sacks, M. D.; Scheiffele, G. W. *Adv. Ceram.* 1986, 19, 175.

(20) Masia, S.; Calvert, P. D.; Rhine, W. E.; Bowen, H. K. *J. Mater. Sci.* 1989, 24, 1907.

(17) Chien, J. C. W.; Uden, P. C.; Fan, J. L. *J. Polym. Sci.: Polym. Chem. Ed.* 1982, 20, 2159.

nitude of this effect may be diminished when physisorbed water is present. Interactions between polymer OH groups and physisorbed water would be expected to be weaker and would be overcome at lower temperature than polymer OH/silanol interactions. On the basis of results presented here and previous results from Masia et al., it can be concluded that the catalytic and inhibitory effects of silica on the decomposition of PVB are dependent on polymer composition, atmospheric environment, and the surface characteristics of the silica. More work in this area is warranted to elucidate the details of these effects.

The primary degradation mechanisms of PVB lead to

polymer residue unsaturation, which increases with increasing temperature. Because this unsaturation is highly conjugated, it is likely that large aromatic structures are formed on silica surfaces at high temperature. Subsequent carbonization of these species might leave regions in the silica in which carbon residue interferes with sintering. The result of this interference could be ceramic defects in the form of voids at locations where Si-O-C bonds were previously formed.

Acknowledgment. Support for this work from Hitachi, Ltd., is gratefully acknowledged.

Liquid-Crystal Behavior in Ionic Complexes of Silver(I): Molecular Structure-Mesogenic Activity Relationship

M. Marcos, M. B. Ros, and J. L. Serrano*

Química Orgánica, Instituto de Ciencia de Materiales de Aragón, Universidad de Zaragoza—C.S.I.C., 50009-Zaragoza, Spain

M. A. Esteruelas, E. Sola, and L. A. Oro

Química Inorgánica, Instituto de Ciencia de Materiales de Aragón, Universidad de Zaragoza—C.S.I.C., 50009-Zaragoza, Spain

J. Barberá

Laboratoire de Physique des Solides, Bâtiment 510, Université Paris-Sud, 91405 Orsay, France

Received July 12, 1990

The liquid-crystal behavior of four series of ionic complexes of silver(I) with structure $[AgL_2]^+X^-$ have been investigated by using differential scanning calorimetry (DSC), optical microscopy, and X-ray diffraction techniques. Two different nonmesogenic pyridine derivatives, $NC_5H_4CH=NC_6H_4OC_nH_{2n+1}$ and $NC_5H_4COOC_6H_4OC_nH_{2n+1}$, were used as ligands (L) and four anions, BF_4^- , $CF_3SO_3^-$, NO_3^- , and PF_6^- , as counterions (X^-). The influence of both the organic ligand and counterion on the liquid-crystal properties of these complexes was studied. These complexes displayed mesogenic behavior identical with that exhibited by typical calamitic liquid crystals. Some of the complexes exhibited additional stable phases between the low-temperature solid phase and the liquid-crystalline phase. A comparative study has shown that pyridinecarboxylate derivatives show higher transition temperatures and wider mesophase ranges than similar imine derivatives. With regard to counterions, the less voluminous the anion, the broader the mesophase range and the lower the melting point.

Introduction

Over the past few years numerous mesogenic molecules containing metals in their structure have been described. These compounds have the usual properties of liquid crystals, but also they can exhibit other special properties due to the presence of metals, as the mesophase allows an ordered distribution of the metal atoms and their electronic environment. As a result, new theoretical studies¹⁻⁴ and

possible practical applications⁵⁻¹⁰ are opening up for these compounds.

In general, the metallo mesogenic compounds described so far contain a liquid-crystal ligand. Recently we described the preparation of rhodium and iridium liquid-

- (1) Marshall, K. L.; Jacobs, S. D. *Mol. Cryst. Liq. Cryst.* **1985**, *159*, 181.
- (2) Giroud-Godquin, A. M.; Sigoud, G.; Achard, M. F.; Hardouin, F. *J. Phys. Lett.* **1984**, *45*, L387. Giroud-Godquin, A. M.; Marchon, J. C.; Guillon, D.; Skoulios, A. *J. Phys. Chem.* **1986**, *90*, 5502.
- (3) Piechocki, C.; Boulon, J. C.; Simon, J. *Mol. Cryst. Liq. Cryst.* **1987**, *149*, 115.
- (4) Chandrasekhar, S.; Sadashiva, B. K.; Ratna, B. R.; Raja, N. V. *Pramana J. Phys.* **1988**, *30*, L491, and references therein.

- (5) Ghedini, M.; Longeri, M.; Bartolino, R. *Mol. Cryst. Liq. Cryst.* **1982**, *84*, 207.
- (6) Hunziker, M. Eur. Pat. Appl. Ed. 162,804 (Cl. C07D257/10), 1984.
- (7) Matsushita Electric Industrial Co. Ltd. Jpn. Kokai Tokkyo Koho. Jp. 60 51,777 [85, 51,777] (Cl. C09K19/40).
- (8) Bruce, D. W.; Dunmur, D. A.; Lalinde, E.; Maitlis, P. M.; Styring, P. *Nature (London)* **1986**, *323*, 791, and references therein.
- (9) Bruce, D. W.; Lalinde, E.; Styring, P.; Dunmur, D. A.; Maitlis, P. M. *J. Chem. Soc., Chem. Commun.* **1986**, 581.
- (10) Adams, H.; Bailey, N. A.; Bruce, D. W.; Dhillon, R.; Dunmur, D. A.; Hunt, S. E.; Lalinde, E.; Maggs, A. A.; Orr, R.; Styring, P.; Wragg, M. S.; Maitlis, P. M. *Polyhedron* **1988**, *7*, 1861.